

脓肿分枝杆菌 MBT 结构鉴定与比较演化分析

薛松¹, 范殊璇¹, 史君涵², 傅翔¹, 邓子新¹, 马伟^{*1}

1 上海交通大学生命科学技术学院 微生物代谢国家重点实验室, 上海 200240

2 上海交通大学生命科学技术学院, 上海 200240

薛松, 范殊璇, 史君涵, 傅翔, 邓子新, 马伟. 脓肿分枝杆菌 MBT 结构鉴定与比较演化分析[J]. 微生物学通报, 2022, 49(11): 4848-4859

Xue Song, Fan Shuxuan, Shi Junhan, Fu Xiang, Deng Zixin, Ma Wei. Structural identification and phylogenetic analysis of MBT from *Mycobacteroides abscessus*[J]. Microbiology China, 2022, 49(11): 4848-4859

摘要:【背景】作为临床最常见的非结核条件致病分枝杆菌, 脓肿分枝杆菌(*Mycobacteroides abscessus*)因其天然、多耐药等特性成为目前临床治疗的一大挑战。作为分枝杆菌限制性营养元素——铁摄取的关键系统, 分枝杆菌素(mycobactin, MBT)、羧基分枝杆菌素(carboxymycobactin, cMBT)与病原分枝杆菌的毒力、耐药等密切相关。【目的】丰富分枝杆菌 MBT、cMBT 结构数据, 探究 MBT 在致病分枝杆菌起源过程中的演化规律。【方法】在 MALDI-TOF-MS 与 FT-MS/MS 解析脓肿 MBT、cMBT 结构的基础上, 进一步开展其活性分析与生物合成基因簇比较基因组分析。【结果】虽然脓肿分枝杆菌 MBT、cMBT 母核修饰模式与海洋分枝杆菌最相似, R1、R2、R3、R5 等位置的修饰完全相同, 而且脂肪酸链均位于 R4 位置; 但脂肪酸链长度不同[C10–17 (MBT)、C4–8 (cMBT)], 为新结构。Fe-cMBT 不仅以浓度依赖方式促进脓肿分枝杆菌生长, 而且利用效率显著高于 FeCl₃, 相关结果表明 MBT-cMBT 是脓肿分枝杆菌高效获取铁元素的关键系统。与 MBT 结构结果一致, *mbt-1* 基因簇共线性分析及 *mbt-1*、*mbt-2* 系统发育分析结果均表明脓肿分枝杆菌与海洋分枝杆菌(*M. marinum*)亲缘关系最近, 而非结核分枝杆菌(*M. tuberculosis*)或耻垢分枝杆菌(*M. smegmatis*) (基于 16S rRNA 基因序列分析)。进一步分析发现, *M. marinum*、*M. tuberculosis*、*M. bovis* 等病原分枝杆菌脂肪酸链长度变化范围仅 4 C, 而 *M. abscessus*、*M. fortuitum*、*M. avium* 和 *M. smegmatis* 等条件致病与非致病菌的脂肪酸链长度变化范围为 7–11 C, 暗示 MBT 同系物脂肪酸链长

基金项目: 2021 上海大学生科技创新创业支持项目(AX-2111); 上海科技发展基金会项目; 上海交通大学多学科交叉项目培育(转化)(YG2021QN38); 科技部重点专项(2018YFE0102400)

Supported by: Shanghai Science and Technology Innovation and Entrepreneurship Support Project for Graduates in 2021 (AX-2111); Shanghai Science and Technology Development Foundation; Transformation of Shanghai Jiao Tong University Multidisciplinary Project (YG2021QN38); Key Project of Ministry of Science and Technology (2018YFE0102400)

*Corresponding author: E-mail: wma@sjtu.edu.cn

Received: 2022-04-17; Accepted: 2022-07-06; Published online: 2022-07-14

度变化范围与分枝杆菌不同生活方式、环境之间可能存在关联。【结论】作为获取铁元素的关键系统, 具有独特结构的脓肿分枝杆菌 MBT-cMBT 在致病、耐药等方面的作用及起源、演化规律值得深入研究。

关键词: 脓肿分枝杆菌; 铁载体; 分枝杆菌素; 羧基分枝杆菌素; 系统发育

Structural identification and phylogenetic analysis of MBT from *Mycobacteroides abscessus*

XUE Song¹, FAN Shuxuan¹, SHI Junhan², FU Xiang¹, DENG Zixin¹, MA Wei^{*1}

¹ State Key Laboratory of Microbial Metabolism, School of Life Sciences and Biotechnology, Shanghai Jiao Tong University, Shanghai 200240, China

² School of Life Sciences and Biotechnology, Shanghai Jiao Tong University, Shanghai 200240, China

Abstract: [Background] As one of the common non-tuberculous conditionally pathogenic mycobacteria, *Mycobacteroides abscessus* is a major clinical challenge because of its natural multi-drug resistance. Mycobactin (MBT) and carboxymycobactin (cMBT), the crucial systems for mycobacteria to acquire iron, one of the limiting nutrients, are closely associated with virulence and drug resistance. [Objective] To reveal the structure of MBT in *M. abscessus* and explore the evolution of MBT in pathogenic mycobacteria. [Methods] The structures of MBT and cMBT were analyzed by MALDI-TOF-MS and FT-MS/MS. Further, the biological activities of MBT and cMBT were determined. The MBT biosynthesis gene clusters were compared between *M. abscessus* and several representative mycobacteria. [Results] *M. abscessus* and *M. marinum* had similar modification patterns of MBT and cMBT core structure. In particular, the modifying groups at R1, R2, R3, and R5 were exactly the same, and the fatty acid chains were both located at R4. However, the MBT and cMBT of *M. abscessus* are a new structure because of the different lengths of the fatty acid chains (10–17 C for MBT and 4–8 C for cMBT). The growth of *M. abscessus* in iron-deprived media could be significantly recovered by supplying with Fe-cMBT in a dosage-dependent manner, and *M. abscessus* can much efficiently absorb Fe-cMBT than FeCl₃, which proved that MBT-cMBT system was vital for *M. abscessus* to acquire iron from the environment. Synteny and phylogenetic analysis of the MBT biosynthetic gene cluster *mbt-1* showed that *M. abscessus* was closely related to *M. marinum* rather than *M. tuberculosis* and *M. smegmatis* (referring to 16S rRNA gene phylogenetic tree). This result is consistent with that based on the structure of MBT. Further analysis revealed that the variation range of the fatty acid chain length of pathogenic mycobacteria such as *M. marinum*, *M. tuberculosis*, and *M. bovis* was only 4 C, while that of conditionally pathogenic and non-pathogenic bacteria such as *M. abscessus*, *M. fortuitum*, *M. avium*, and *M. smegmatis* was 7–11 C, which suggested that the range variation of fatty acid chain length of MBT might be associated with the lifestyles and habitats of mycobacteria. [Conclusion] As an important system for obtaining iron with unique structure, *M. abscessus* MBT deserved further study, especially its roles in pathogenesis and drug resistance, as well as its evolution in pathogenic mycobacteria.

Keywords: *Mycobacteroides abscessus*; siderophore; mycobactin; carboxymycobactin; phylogeny

脓肿分枝杆菌是非结核条件致病分枝杆菌(non-tuberculosis mycobacteria, NTM),以囊性纤维化、支气管扩张、艾滋病患者及器官移植、老年等免疫低下人群为主要易感群体^[1-2],可感染肺部、关节及皮肤等部位^[3-4]。在发达国家,临床上脓肿分枝杆菌占快生长非结核分枝杆菌肺部感染的80%且呈逐年上升趋势^[5]。由于独特的细胞壁结构与代谢机制^[6-7],其能够抵御巨噬细胞和中性粒细胞等免疫细胞攻击,加之天然多耐药^[8],导致其治疗周期长、疗效不理想^[9]。例如,囊性纤维化患者6个月以上的长周期治疗,治愈率也仅有30%–50%^[10]。

铁元素参与细菌的呼吸、DNA合成及自由基清除等重要过程^[11],因此与细菌侵染、生长、抵抗巨噬细胞等免疫细胞攻击^[12-13]及抗生素耐药^[14-15]等密切相关。在生理pH条件下, Fe^{3+} 溶解度比细菌生长所需浓度低3–4个数量级^[16],在炎症情况下,非特异免疫细胞可以局部产生乳铁蛋白、铁调素等抑制感染部位细菌对铁的获取^[17],因此,铁限制是人类等宿主抵御病原菌感染的重要防御手段^[18-19]。然而病原菌则通过合成与铁离子亲和性极高的铁载体从宿主转铁蛋白等蛋白中夺取铁^[20]。针对结核分枝杆菌的研究发现,铁载体合成缺陷菌株在巨噬细胞中的生长受到显著抑制^[21];而铁载体受体蛋白FecB缺失导致其对万古霉素、美罗培南等多种抗生素敏感性增强^[22]。

正是由于铁载体重要功能与作用,目前,有研究将抗生素与病原菌铁载体偶联,以提高抗生素进入菌体效率从而提升菌体内抗生素浓度,即所谓的特洛伊木马策略^[23-24],以及针对铁载体合成关键酶开发抑制剂^[25]等已成为抗生素研发热点。例如体外实验表明,3-苯基丙烯酸酯类化合物通过竞争性底物抑制结核分枝杆菌铁载体合成途径中的关键酶从而限制其

生长^[26]。

在缺铁环境中,分枝杆菌主要通过合成疏水的分枝杆菌素(mycobactin, MBT)^[27]和亲水的羧基分枝杆菌素(carboxymycobactin, cMBT)高效吸收铁^[28]。以结核分枝杆菌为例,细胞外的cMBT螯合铁后,通过HupB将 Fe^{3+} 转移给位于周质空间中的MBT,Fe-MBT通过铁载体转运蛋白IrtAB将铁元素转运至细胞内,但铁元素从HupB转移到MBT的机制尚不清楚^[29]。结核分枝杆菌的MBT生物合成基因簇由*mbt-1*和*mbt-2*两部分组成,*mbt-1*基因簇由*mbtA–mbtJ*等10个基因构成,主要负责MBT母核的合成^[30]。*mbt-2*基因簇包括*mbtK–mbtN*等4个基因,负责MBT疏水脂肪酸链的组装^[31]。结核、耻垢等菌的MBT相关研究表明,分枝杆菌MBT、cMBT母核结构高度保守(图1),而母核苯环上R₁–R₅等位置修饰模式及脂肪酸链长度^[29,31]具有物种特异性。在所有MBT结构已被研究的分枝杆菌中,除海洋分枝杆菌脂肪酸链位于R₄外^[32],结核、耻垢等其他分枝杆菌脂肪酸链均位于

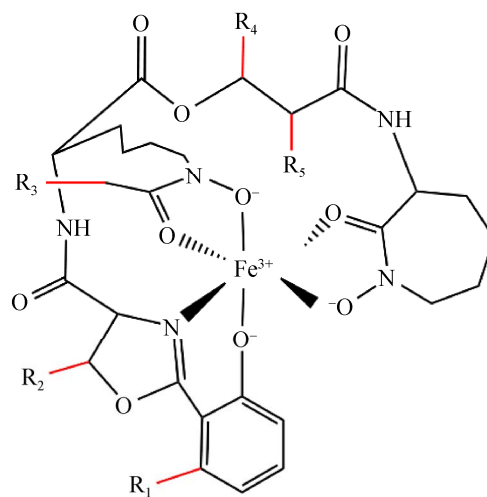


图1 分枝杆菌素母核结构与关键修饰基团
Figure 1 Schematic representation of the core structure and key modifications of mycobactins/carboxymycobactin from mycobacteria.

R3^[29]。脂肪酸链为 MBT 固着于细胞膜及 IrtAB 转运 MBT 所必需^[33]。研究发现, 各菌均会合成一系列脂肪酸链长短不一的 MBT 和 cMBT, 如结核 MBT 为 C17–20^[29,34], 而耻垢为 C9–19^[29,35], 但其生物学功能与意义尚不清楚。

针对在水体、人体组织等多种环境中均可生长且具有条件致病性的脓肿分枝杆菌的 MBT 结构的研究, 无疑将对于揭示分枝杆菌铁元素获取机制具有重要意义。

1 材料与方 法

1.1 菌株与培养基

菌株: *M. abscessus* ATCC 19977 菌株由本实验室保存。

培养基: *M. abscessus* 采用 7H9^[36]于 37 °C、120 r/min 培养 2–3 d 至指定 OD_{600} 值, 用于后续实验。用于铁载体提取时, 采用除铁最低营养培养基^[32], 经除铁最低营养培养基中传代 2 次之后, 以 0.5% 比例接种至 500 mL 除铁最低营养培养基中培养, 于 37 °C、120 r/min 培养 14 d, 25 °C、6 000 r/min 离心 30 min, 分别取上清和沉淀用于 cMBT 与 MBT 提取。

1.2 实验方法

1.2.1 铁载体提取

M. abscessus 铁载体提取参照文献^[32]方法进行。

1.2.2 质谱分析

MALDI-TOF-MS: 将溶于乙腈中的铁载体与 HCCA 等体积混合, 氮气吹干后, 进行分析, m/z 检测范围为 700–1 100。

FT-MS/MS: 鞘层气体流速: 5 250 kPa, 辅助气流速: 1 750 kPa, 毛细管温度: 350 °C, 全扫描模式分辨率: 120 000, MS/MS 扫描模式分辨率: 7 500, 喷雾电压: 4.0 kV (阳离子)或 –3.8 kV (阴离子)。

1.2.3 Fe-cMBT 对缺铁脓肿分枝杆菌生长恢复作用分析

经缺乏铁元素的最低营养培养基连续培养 2 代后, 按 1% 接种于按指定浓度添加 Fe-cMBT、FeCl₃ 或等体积 ddH₂O 的最低营养培养基, 37 °C、120 r/min 培养 4 d, 每 12 h 测量 OD_{600} 值。

1.2.4 系统发育学分析

自 NCBI (<https://www.ncbi.nlm.nih.gov/>) 与 KEGG (<https://www.kegg.jp/kegg/kegg2.html>) 公共数据库下载 *M. tuberculosis* H37Rv、*M. smegmatis* MC2 155、*M. abscessus* ATCC 19977、*M. marinum* M、*M. canettii* CIPT 140010059、*M. bovis* AF2122/97、*M. avium* 2285 (R)、*M. fortuitum* subsp. *fortuitum* ATCC 6841 等菌株的 MBT 生物合成蛋白序列, 对未注释蛋白采用 *M. tuberculosis* 的相关蛋白对目标菌蛋白数据集进行 BLASTp, 相似度最高、 E -value < 10^{-20} 的比对结果认作同源蛋白, 具体序列 accession 号如表 1 所示。使用 MEGA X^[37] 软件的最大似然方法进行系统发育树构建, 通过 1 000 次自举重复评估节点支持。

1.2.5 统计学分析

实验结果为 3 次独立实验平均值, 采用 GraphPad Prism 软件 paired t -test 模块进行组间差异统计学分析, $P < 0.05$ 认定为差异显著。

2 结果与分析

2.1 脓肿分枝杆菌分枝杆菌素的结构

从 MALDI-TOF-MS 谱图(图 2)中可以观察到 MBT、Fe-MBT 与 cMBT、Fe-cMBT 的分子离子峰, 表明两者均具有与 Fe³⁺ 的结合能力。MBT 的脂肪酸链长度变化范围为 C10–17, 其中高丰度同系物链长为 C10–13、C15、C17, 详见图 2A。从图 2B 中可以看到, cMBT 脂肪酸链长度大约从 C4–8 不等, 高丰度组分的链长为 C5–8。

表 1 用于系统发育分析的 *mbt* 基因簇编码蛋白登录号Table 1 Accession No. of *mbt* gene cluster coding proteins for phylogenetic analysis

Coding protein	<i>M. abscessus</i>	<i>M. avium</i>	<i>M. canetti</i>	<i>M. marinum</i>
MbtA	WP_005088755.1	EUA36076.1	WP_014001248.1	ACC42114.1
MbtB	WP_005110650.1	EUA36980.1	WP_014001247.1	WP_012395305.1
MbtC	WP_005080165.1	EUA39465.1	WP_003412278.1	WP_012395309.1
MbtD	WP_005110643.1	EUA38842.1	WP_014001246.1	WP_012395310.1
MbtE	WP_005110645.1	EUA38931.1	WP_041180111.1	WP_012395307.1
MbtF	WP_005110647.1	EUA39107.1	WP_041180276.1	WP_012395306.1
MbtG	WP_005086054.1	EUA37716.1	WP_014001243.1	WP_041324786.1
MbtH	CAM62331.1	EUA36332.1	WP_003412265.1	WP_011741377.1
MbtI	WP_005096783.1	EUA39884.1	WP_014001250.1	ACC42122.1
MbtJ	WP_005098458.1	EUA39656.1	WP_041180112.1	WP_012395313.1
MbtK	WP_005076691.1	EUA40352.1	WP_003406956.1	WP_012393422.1
MbtM	CAM64737.1	EUA36117.1	WP_003406950.1	WP_237708340.1
MbtN	WP_005082911.1	EUA39862.1	WP_003406953.1	WP_012396082.1
Coding protein	<i>M. smegmatis</i>	<i>M. tuberculosis</i>	<i>M. bovis</i>	<i>M. fortuitum</i>
MbtA	ABK70627.1	WP_003412282.1	WP_003412282.1	CRL54347.1
MbtB	WP_011729889.1	WP_003899299.1	WP_010950705.1	CRL56150.1
MbtC	WP_011729888.1	WP_003412278.1	WP_003412278.1	EJZ16316.1
MbtD	ABK75467.1	WP_003412277.1	WP_003412277.1	WP_003879643.1
MbtE	ABK72785.1	WP_003899297.1	WP_003899297.1	WP_051018853.1
MbtF	AFP40852.1	WP_023637453.1	WP_031657277.1	WP_003879641.1
MbtG	WP_011729884.1	WP_003899296.1	WP_003899296.1	WP_003879640.1
MbtH	WP_011729883.1	WP_003916994.1	WP_003412265.1	WP_003884873.1
MbtI	WP_011729893.1	WP_003412287.1	WP_003412287.1	EJZ16323.1
MbtJ	WP_011726795.1	WP_003899300.1	WP_003899300.1	WP_038563859.1
MbtK	WP_011728178.1	WP_003406956.1	WP_003406956.1	WP_003879974.1
MbtM	ABK75882.1	WP_003406950.1	WP_003406950.1	WP_003879972.1
MbtN	ABK70771.1	WP_003406953.1	WP_003406953.1	WP_003881372.1

高分辨 FT-MS/MS 二级质谱谱图分析分别确定了 *M. abscessus* 的 MBT、cMBT 的 R1、R2、R3、R4、R5 等修饰基团(表 2)。值得注意的是, 脓肿分枝杆菌脂肪酸链位于 R4 位置, 即母核的中心酯基团与酰胺基团之间(图 3)。

2.2 Fe-cMBT 促进脓肿分枝杆菌在缺铁培养基中的生长

从图 4 中可以看到, Fe-cMBT 可显著促进 *M. abscessus* 生长, 培养至 72 h, 添加 1、5 和 10 $\mu\text{mol/L}$ 的 Fe-cMBT 组 OD_{600} 值分别比对照

组高 37.8%、120.7%和 178.5%, 84 h 后分别高 10.7%、56.0%和 105.2%, 96 h 后分别高 9.4%、61.9%和 100.8% (图 4)。

对比 cMBT 螯合铁与无机铁可以发现, 虽然铁离子较为丰富时(如 10 $\mu\text{mol/L}$), Fe-cMBT 与 FeCl_3 组无显著差异(结果未展示), 但是 5 $\mu\text{mol/L}$ 铁离子浓度下, 培养至 60 h 时 Fe-cMBT 组 OD_{600} 值高于 FeCl_3 组 21.1% ($P=0.0124$), 72 h 时高 14.7% ($P=0.0039$), 84 h 高 16.7% ($P=0.0527$), 96 h 高 15.2% ($P=0.1127$)。

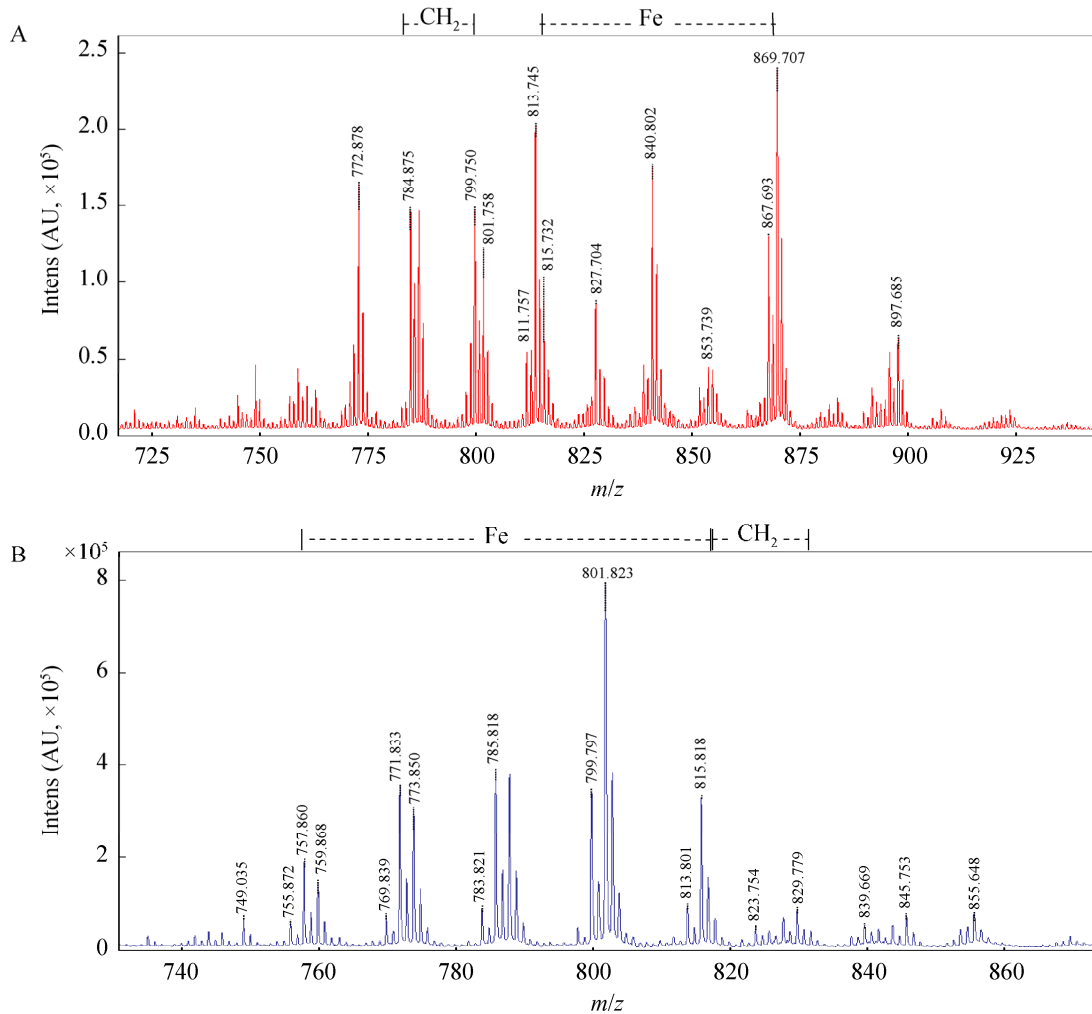


图2 *Mycobacteroides abscessus* MBT 与 cMBT 的 MALDI-TOF-MS 谱图 A: MBT 谱图; B: cMBT 谱图
Figure 2 MALDI-TOF-MS mass spectrum of MBT and cMBT from *Mycobacteroides abscessus*. A: Mass spectrum of MBT; B: Mass spectrum of cMBT.

2.3 分枝杆菌典型菌 MBT 合成基因簇比较基因组分析

2.3.1 分枝杆菌家族 MBT 合成基因簇共线性分析

从图 5 中可以看到, 虽然 *M. smegmatis* *mbt-1* 基因簇各成员在基因组中的排列方向与 *M. tuberculosis*、*M. canetti* 和 *M. bovis* 等菌相反, *M. fortuitum* 的 *mbtB* 与 *mbtC* 间插入了 2 个与 MBT 合成无关基因及 *M. avium* 的 *mbtE* 基因的长度比其他分枝杆菌的 *mbtE* 长约 1 500 bp,

但是这些菌 *mbt-1* 基因簇成员均按 *mbtA*–*mbtH* 顺序排列。*M. abscessus* 和 *M. marinum* 的 *mbt-1* 基因簇中仅 D-C-E-F-B 的排列顺序相同, 其他基因排列顺序并不相同; 而且 *M. abscessus* 的 *mbt-1* 由两段构成, 中间相隔 100 多个基因且各包含一个 *mbtE*。

观察 *mbt-2* 相关基因在基因组中的分布可以看出, *M. tuberculosis*、*M. fortuitum*、*M. smegmatis*、*M. bovis* 和 *M. canetti* 等菌的 *mbtK*、*mbtL*、*mbtM*、*mbtN* 在基因组中连续排列; *M. avium* 的 *mbtL*

表 2 分枝杆菌 MBT/cMBT 母核修饰基团

Table 2 Variable residues of different mycobacteria's MBT/cMBT

Strains	R1 MBT/cMBT	R2 MBT/cMBT	R3 MBT/cMBT	R4 MBT/cMBT	R5 MBT/cMBT	Pathogenicity and growth speed	Reference
<i>M. abscessus</i>	H	CH ₃	CH ₃	C10-17/C4-8 or C3-7	CH ₃	Opportunistic Pathogens (RGM)	This Study
<i>M. tuberculosis</i>	H	H/H,CH ₃	C17-20/C3-9 or C1-9	CH ₃	H	True Pathogens	[29-30]
<i>M. smegmatis</i>	H	H/H,CH ₃	C9-19/Not available	CH ₃	H	Saprophytes (RGM)	[29,31]
<i>M. bovis</i>	H	H/H,CH ₃	C17-20/C3-9 or C1-9	CH ₃	H	True Pathogens	[29-30]
<i>M. avium</i>	H	CH ₃	C11-14,18/C1-9 or C2-5	CH ₂ CH ₃	CH ₃	Opportunistic Pathogens (SGM)	[29-30]
<i>M. fortuitum</i>	CH ₃ /Not available	CH ₃ /Not available	C9-17/Not available	CH ₃ /Not available	H/Not available	Opportunistic Pathogens (RGM)	[29]
<i>M. marinum</i>	H	CH ₃	CH ₃	C15-18/C7-9 or C3-6	CH ₃	True Pathogens (SGM)	[32]

注: cMBT 的 R3 或 R4 末端中有羧基(RCOOH)和甲酯(RCOOCH₃)两种形式。RGM: Rapidly-growing mycobacteria; SGM: Slowly-growing mycobacteria。所有的病原性分枝杆菌均为慢生长型

Note: The R3 or R4 terminus of cMBT have two types: carboxyl (RCOOH) and methyl ester (RCOOCH₃). RGM: Rapidly-growing mycobacteria; SGM: Slowly-growing mycobacteria. All pathogenic mycobacteria are slowly-growing type.

独立, 其余 3 个基因连续排列; 而 *M. abscessus* 和 *M. marinum* 不仅 *mbtL* 缺失, 其余 3 个基因均分散排列(表 3)。

2.3.2 分枝杆菌代表菌 *mbt-1* 基因簇系统发育分析

对脓肿等菌的 *mbt-1* 基因簇基因编码的蛋白进行系统发育分析发现, *M. tuberculosis* 与 *M. canetti*、*M. bovis* 最相似, *M. fortuitum* 与 *M. smegmatis* 最相似, 而 *M. abscessus* 与 *M. marinum* 最相似且独立成簇(图 6A)。

基于 MbtK、MbtM 与 MbtN 的 *mbt-2* 系统发育分析发现(*M. abscessus* 与 *M. marinum* 无 *mbtL*), *mbt-2* 进化树结构与 *mbt-1* 相似, *M. abscessus* 与 *M. marinum* 亲缘关系最近(图 6B)。

3 讨论与结论

本研究对 MBT 与 cMBT 结构鉴定发现, *M. abscessus* MBT、cMBT 母核 R1、R2、R3、

R5 等位置的修饰模式与海洋分枝杆菌相同, 脂肪酸链也位于 R4 位置; 但 MBT、cMBT 脂肪酸链长度分别为 C10-17 和 C4-8, 该结构未见报道。Fe-cMBT 生物活性分析发现, cMBT 以浓度依赖方式促进缺铁 *M. abscessus* 生长, 而且 *M. abscessus* 对 cMBT 利用效率显著高于无机铁。上述实验结果表明, MBT-cMBT 系统是 *M. abscessus* 高效吸收环境铁元素的关键系统。

在已有 MBT 结构报道的分枝杆菌中, *M. abscessus* MBT 母核修饰模式与慢生长型的 *M. marinum* 最接近, 但脂肪酸链长度及变化范围又与之存在明显差异。对它们进行比较分析可以发现, *M. marinum*、*M. tuberculosis*、*M. bovis* 等慢生长型、病原分枝杆菌^[30,38]脂肪酸链长度变化范围仅 4 个碳, 而条件致病菌, 无论是慢生长型的 *M. avium* 还是快生长型的 *M. abscessus* 与 *M. fortuitum* 及非致病菌 *M. smegmatis* 等条件致病菌的脂肪酸链长度变化

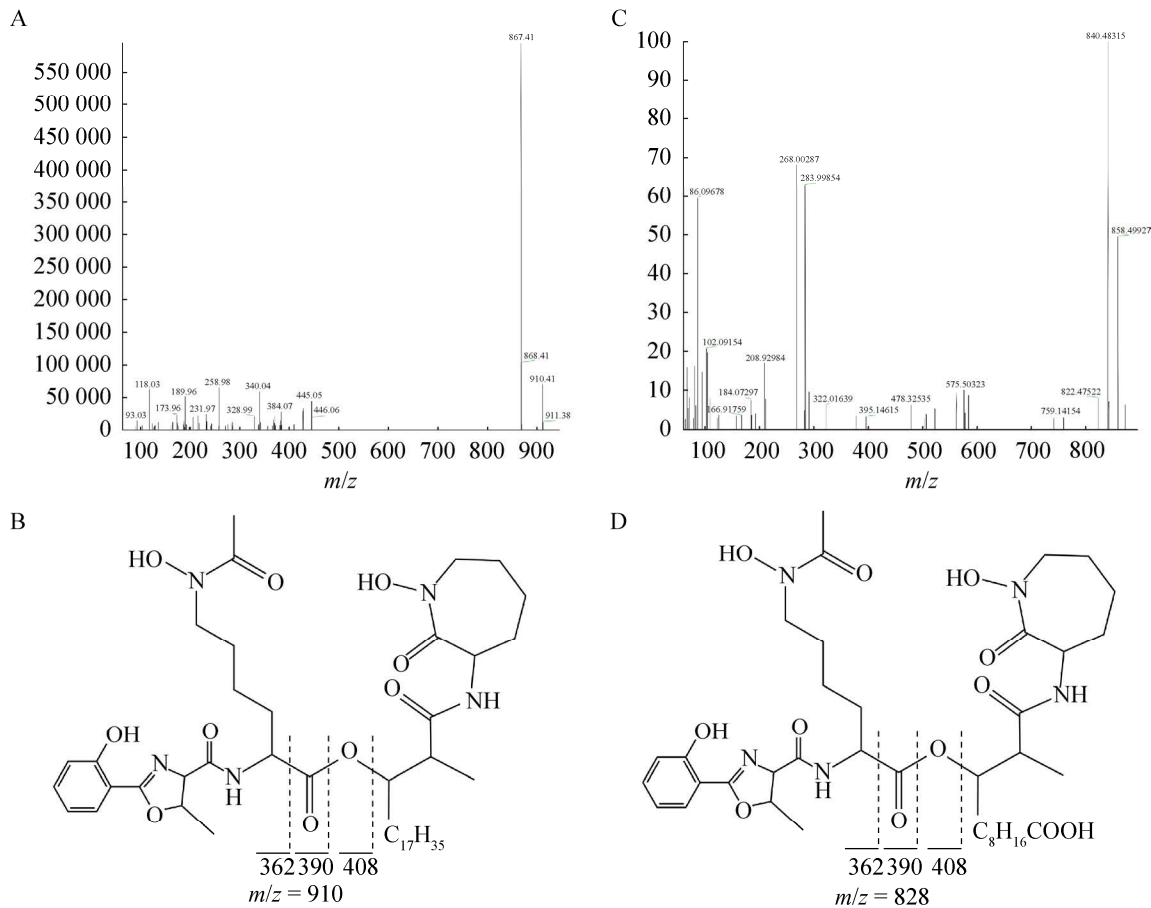


图 3 *Mycobacteroides abscessus* MBT 和 cMBT 的 FT-MS/MS 谱图与推测结构 A 和 B: MBT 质谱谱图及推测结构; C 和 D: cMBT 质谱谱图与结构

Figure 3 FT-MS/MS mass spectrum of MBT and cMBT from *Mycobacteroides abscessus*. A, B: Mass spectrum and speculated structure of MBT; C, D: Mass spectrum and speculated structure of cMBT.

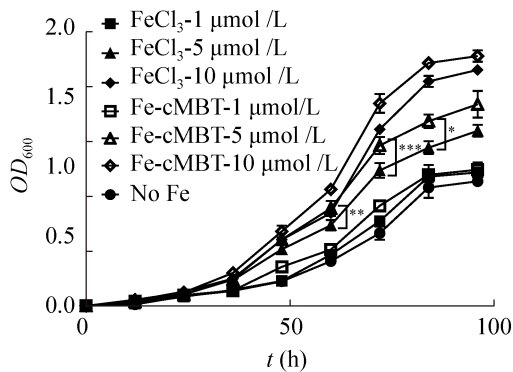


图 4 Fe-cMBT 对缺铁条件下脓肿分枝杆菌生长作用

Figure 4 Effect of Fe-cMBT on the growth of *M. abscessus* in iron deprivation. *: $P < 0.1$; **: $P < 0.05$; ***: $P < 0.01$.

范围达 C7–11。即致病菌脂肪酸链长度变化范围远小于条件致病菌与环境菌，而且更倾向于合成脂肪酸侧链较长的 MBT。我们推测，具有较大变化范围脂肪酸链的 MBT 或许更有利于细菌从多样、多变环境中获取铁；而长但变化范围小的脂肪酸链或有利于病原分枝杆菌从较为稳定宿主环境，如人体中高效夺取铁元素。

MBT 合成基因簇无论是共线性还是系统发育树均为 *M. abscessus* 与 *M. marinum* 最相似(图 5 和图 6)，该结果与基于 16S rRNA 基因序列的亲缘关系分析结果完全不同^[39]，我们推测两者 MBT 生物合成基因簇发生过水平转移事件。

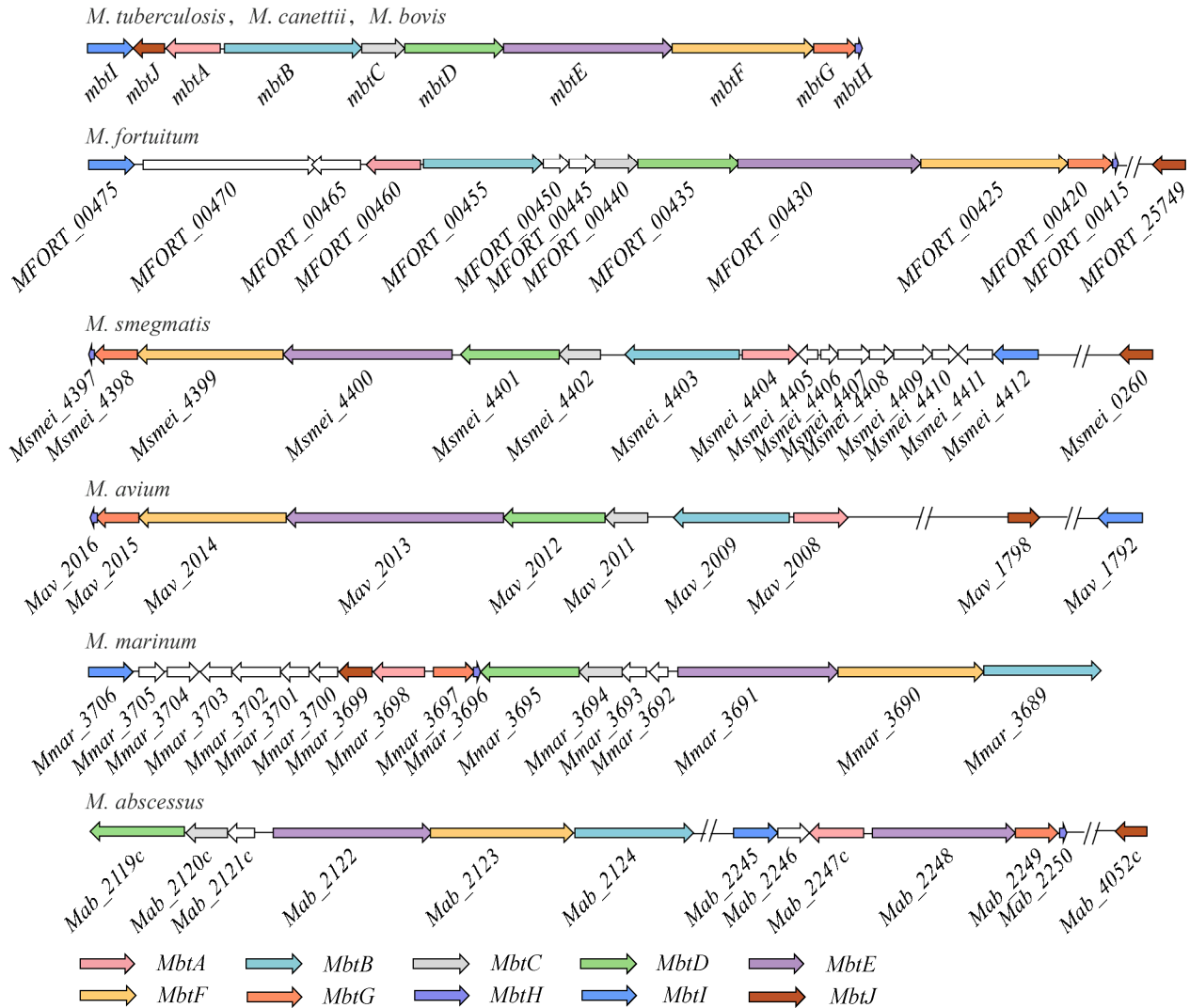


图 5 分枝杆菌家族不同菌株的 *mbt-1* 合成基因簇的排列模式 使用不同的颜色标注出了 *mbtA*–*mbtJ*。从上至下分别为：结核分枝杆菌、偶发分枝杆菌、耻垢分枝杆菌、鸟分枝杆菌、海洋分枝杆菌和脓肿分枝杆菌。卡内蒂分枝杆菌、牛分枝杆菌的基因排列模式与结核分枝杆菌完全相同

Figure 5 Alignment patterns of *mbt-1* synthesis gene clusters in different strains of the mycobacterium family. The *mbtA*–*mbtJ* genes are labeled using different colors from top to bottom: *M. tuberculosis*, *M. fortuitum*, *M. smegmatis*, *M. avium*, *M. marinum*, *M. abscessus*. The gene clusters alignment patterns of *M. canetti* and *M. bovis* are same as *M. tuberculosis*.

M. tuberculosis 脂肪酸链位于 R3 位置，其 MBT 生物合成研究发现，MbtMN 首先将脂肪酸链转移到 *mbtL* 编码的酰基载体蛋白上并活化^[40]，然后由 *mbtK* 编码的 N-酰基转移酶通过转酰基反应连接到母核的氨基上，最终由 MbtG 通过酰胺基羟基化等反应生成异羟肟酸^[33]。然

而 *M. abscessus* 与 *M. marinum* 的脂肪酸链直接连接在碳链上(R4)，这就意味着脂肪酸链是以完全不同的方式添加或母核合成方式与结核等菌不同。同时，脂肪酸链着生于 R4 位置时，螯合铁的 MBT 母核与细胞膜距离比 R3 着生方式更远(图 1)。2 种方式对铁元素获取效率是否存

表 3 不同分枝杆菌 *mbt-2* 基因簇基因构成Table 3 Genes in *mbt-2* cluster from different mycobacteria

Strains	<i>mbtK</i>	<i>mbtL</i>	<i>mbtM</i>	<i>mbtN</i>
<i>M. abscessus</i>	<i>Mab_3125c</i>	–	<i>Mab_4668c</i>	<i>Mab_1070c</i>
<i>M. avium</i>	<i>Mav_2875</i>	<i>Mav_0029</i>	<i>Mav_2874</i>	<i>Mav_2876</i>
<i>M. canettii</i>	<i>Mcan_RS07180</i>	<i>Mcan_RS07165</i>	<i>Mcan_RS07170</i>	<i>Mcan_RS07175</i>
<i>M. marinum</i>	<i>Mmar_1587</i>	–	<i>Mmar_3272</i>	<i>Mmar_4532</i>
<i>M. smegmatis</i>	<i>Msmei_2080</i>	<i>Msmei_2083</i>	<i>Msmei_2082</i>	<i>Msmei_2081</i>
<i>M. tuberculosis</i>	<i>Rv1347c</i>	<i>Rv1344</i>	<i>Rv1345</i>	<i>Rv1346</i>
<i>M. bovis</i>	<i>BQ2027_RS07055</i>	<i>BQ2027_RS07040</i>	<i>BQ2027_RS07045</i>	<i>BQ2027_RS07050</i>
<i>M. fortuitum</i>	<i>Mfort_06229</i>	<i>Mfort_06214</i>	<i>Mfort_06219</i>	<i>Mfort_06224</i>

注: –: 通过 BLASTp 比对后无法找到对应的同源基因(E -value $>10^{-20}$)

Note: –: The corresponding homologous gene cannot be found after BLASTp alignment (E -value $>10^{-20}$).

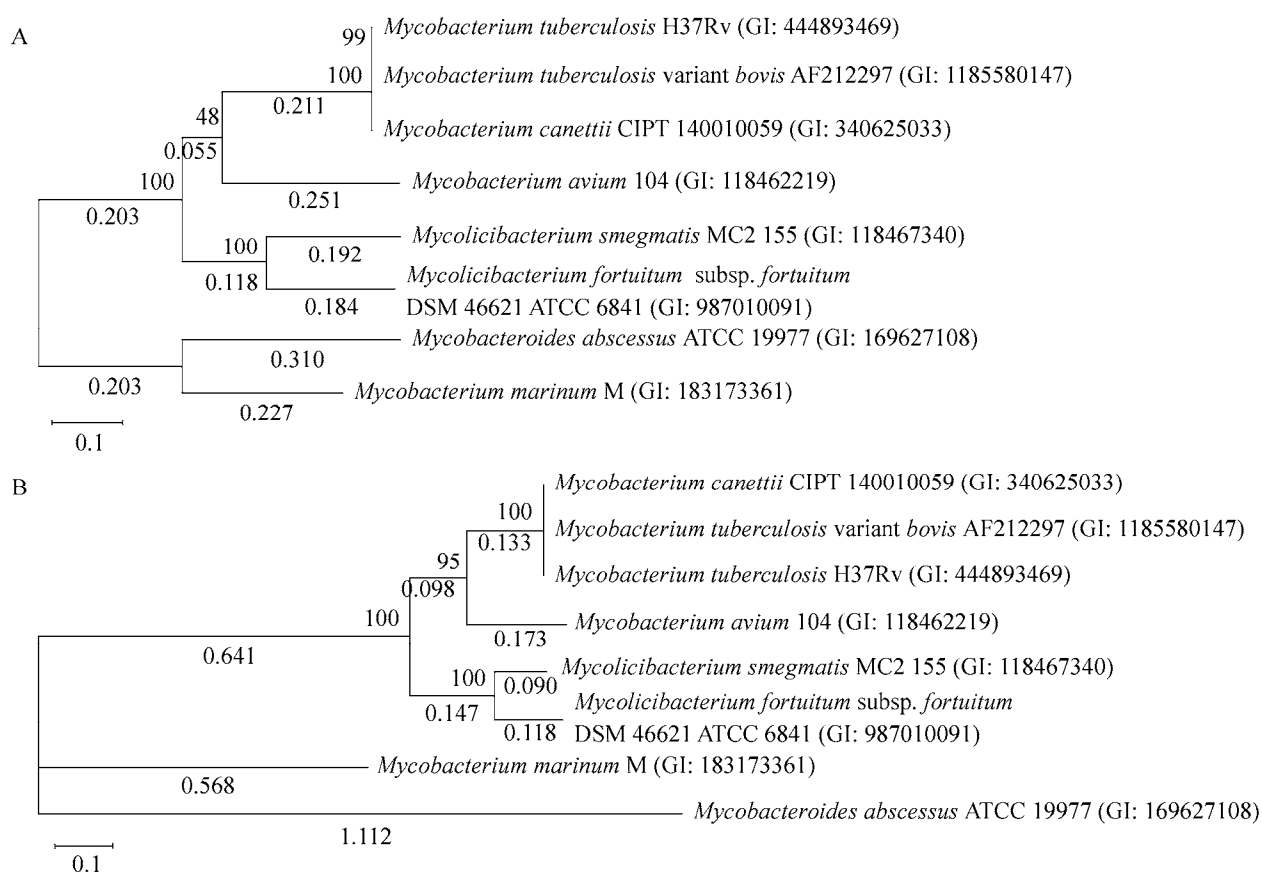


图 6 分枝杆菌代表菌 MBT 合成基因编码蛋白系统发育分析 A: *mbt-1* 系统发育树; B: *mbt-2* 系统发育树。括号中序号为菌株序列的 GenBank 登录号; 分支点处数值为 1 000 次自举验证可信率(百分比值); 系统树枝上数值为其进化距离

Figure 6 Phylogenetic analysis of proteins encoded by MBT synthesis genes from representative mycobacteria. A: Phylogenetic tree of *mbt-1*; B: Phylogenetic tree of *mbt-2*. The number in brackets is the GenBank accession number of the strain; The value at the branch point is the confidence rate (percentage value) of 1 000 times bootstrap verification; The value on the phylogenetic branch is the evolutionary distance.

在影响值得深入研究。

总而言之, MBT 结构解析与功能研究不仅有助于深入阐明分枝杆菌铁获取及致病菌侵染、免疫抵抗、耐药等机制, 更能通过揭示 MBT 在病原分枝杆菌起源过程中的演化规律, 为 *M. abscessus* 治疗方案与药物研发提供有价值的信息。

REFERENCES

- [1] Sapriel G, Konjek J, Orgeur M, Bouri L, Frézal L, Roux AL, Dumas E, Brosch R, Bouchier C, Brisse S, et al. Genome-wide mosaicism within *Mycobacterium abscessus*: evolutionary and epidemiological implications[J]. BMC Genomics, 2016, 17: 118
- [2] Degiacomi G, Sammartino JC, Chiarelli LR, Riabova O, Makarov V, Pasca MR. *Mycobacterium abscessus*, an emerging and worrisome pathogen among cystic fibrosis patients[J]. International Journal of Molecular Sciences, 2019, 20(23): 5868
- [3] De Groote MA, Huitt G. Infections due to rapidly growing *Mycobacteria*[J]. Clinical Infectious Diseases, 2006, 42(12): 1756-1763
- [4] 郝红芬, 张宏丽. 脓肿分枝杆菌肺病抗感染药物治疗研究进展 [J]. 医学理论与实践, 2021, 34(12): 2021-2023, 2017
Hao HF, Zhang HL. Advances in anti-infective drug therapy for *Mycobacterium abscessus* pulmonary disease[J]. The Journal of Medical Theory and Practice, 2021, 34(12): 2021-2023, 2017 (in Chinese)
- [5] Varghese G, Shepherd R, Watt P, Bruce JH. Fatal infection with *Mycobacterium fortuitum* associated with oesophageal achalasia[J]. Thorax, 1988, 43(2): 151-152
- [6] Brennan PJ. Structure, function, and biogenesis of the cell wall of *Mycobacterium tuberculosis*[J]. Tuberculosis, 2003, 83(1/2/3): 91-97
- [7] Daher W, Leclercq LD, Viljoen A, Karam J, Dufrêne YF, Guérardel Y, Kremer L. O-methylation of the glycopeptidolipid acyl chain defines surface hydrophobicity of *Mycobacterium abscessus* and macrophage invasion[J]. ACS Infectious Diseases, 2020, 6(10): 2756-2770
- [8] Yam YK, Alvarez N, Go ML, Dick T. Extreme drug tolerance of *Mycobacterium abscessus* “persisters”[J]. Frontiers in Microbiology, 2020, 11: 359
- [9] Baldwin SL, Larsen SE, Ordway D, Cassell G, Coler RN. The complexities and challenges of preventing and treating nontuberculous mycobacterial diseases[J]. PLoS Neglected Tropical Diseases, 2019, 13(2): e0007083
- [10] Ferro BE, Srivastava S, Deshpande D, Pasipanodya JG, van Soolingen D, Mouton JW, Van Ingen J, Gumbo T. Failure of the amikacin, cefoxitin, and clarithromycin combination regimen for treating pulmonary *Mycobacterium abscessus* infection[J]. Antimicrobial Agents and Chemotherapy, 2016, 60(10): 6374-6376
- [11] Herb M, Schramm M. Functions of ROS in macrophages and antimicrobial immunity[J]. Antioxidants: Basel, Switzerland, 2021, 10(2): 313
- [12] Gokarn K, Pal RB. Activity of siderophores against drug-resistant Gram-positive and Gram-negative bacteria[J]. Infection and Drug Resistance, 2018, 11: 61-75
- [13] Pal R, Hameed S, Fatima Z. Iron deprivation affects drug susceptibilities of *Mycobacteria* targeting membrane integrity[J]. Journal of Pathogens, 2015, 2015: 938523
- [14] Pal R, Hameed S, Kumar P, Singh S, Fatima Z. Understanding lipidomic basis of iron limitation induced chemosensitization of drug-resistant *Mycobacterium tuberculosis*[J]. 3 Biotech, 2019, 9(4): 122
- [15] 李微, 张万江. 微量铁元素在结核病发病机制中作用的研究进展[J]. 细胞与分子免疫学杂志, 2012, 28(5): 554-556
Li W, Zhang WJ. Advances in the role of trace iron in the pathogenesis of tuberculosis[J]. Chinese Journal of Cellular and Molecular Immunology, 2012, 28(5): 554-556 (in Chinese)
- [16] De Serrano LO, Camper AK, Richards AM. An overview of siderophores for iron acquisition in microorganisms living in the extreme[J]. BioMetals, 2016, 29(4): 551-571
- [17] Cassat JE, Skaar EP. Iron in infection and immunity[J]. Cell Host & Microbe, 2013, 13(5): 509-519
- [18] Kochan I. The role of iron in bacterial infections, with special consideration of host-tubercle *Bacillus* interaction[J]. Current Topics in Microbiology and Immunology, 1973, 60: 1-30
- [19] 姜华, 杨秋林. 铁、钙、氢离子在结核分枝杆菌免疫逃逸机制中的相关研究[J]. 微生物学免疫学进展, 2011, 39(1): 62-65
Jiang H, Yang QL. Study on the relevance of iron, calcium and hydrogen ions in the immune escape mechanism of *Mycobacterium tuberculosis*[J]. Progress in Microbiology and Immunology, 2011, 39(1): 62-65 (in Chinese)
- [20] Ratledge C, Dover LG. Iron metabolism in pathogenic bacteria[J]. Annual Review of Microbiology, 2000, 54: 881-941
- [21] De Voss JJ, Rutter K, Schroeder BG, Su H, Zhu Y, Barry

- CE 3rd. The salicylate-derived mycobactin siderophores of *Mycobacterium tuberculosis* are essential for growth in macrophages[J]. Proceedings of the National Academy of Sciences of the United States of America, 2000, 97(3): 1252-1257
- [22] Xu WZ, DeJesus MA, Rücker N, Engelhart CA, Wright MG, Healy C, Lin K, Wang RJ, Park SW, Ioerger TR, et al. Chemical genetic interaction profiling reveals determinants of intrinsic antibiotic resistance in *Mycobacterium tuberculosis*[J]. Antimicrobial Agents and Chemotherapy, 2017, 61(12): e01334-e01317
- [23] Miller MJ, Walz AJ, Zhu H, Wu CR, Moraski G, Möllmann U, Tristani EM, Crumbliss AL, Ferdig MT, Checkley L, et al. Design, synthesis, and study of a mycobactin-artemisinin conjugate that has selective and potent activity against tuberculosis and malaria[J]. Journal of the American Chemical Society, 2011, 133(7): 2076-2079
- [24] 张利, 刘马峰, 程安春. 铁载体-抗生素耦合剂: 一种新型的抗菌制剂[J]. 微生物学通报, 2016, 43(7): 1598-1604
- Zhang L, Liu MF, Cheng AC. Siderophore-antibiotic conjugates: the new antimicrobial agents[J]. Microbiology China, 2016, 43(7): 1598-1604 (in Chinese)
- [25] Patel K, Butala S, Khan T, Suvarna V, Sherje A, Dravyakar B. Mycobacterial siderophore: a review on chemistry and biology of siderophore and its potential as a target for tuberculosis[J]. European Journal of Medicinal Chemistry, 2018, 157: 783-790
- [26] Manos-Turvey A, Cergol KM, Salam NK, Bulloch EMM, Chi G, Pang A, Britton WJ, West NP, Baker EN, Lott JS, et al. Synthesis and evaluation of *M. tuberculosis* salicylate synthase (MbtI) inhibitors designed to probe plasticity in the active site[J]. Organic & Biomolecular Chemistry, 2012, 10(46): 9223
- [27] Snow GA. Isolation and structure of mycobactin T, a growth factor from *Mycobacterium tuberculosis*[J]. The Biochemical Journal, 1965, 97(1): 166-175
- [28] Gobin J, Moore CH, Reeve JR Jr, Wong DK, Gibson BW, Horwitz MA. Iron acquisition by *Mycobacterium tuberculosis*: isolation and characterization of a family of iron-binding exochelins[J]. PNAS, 1995, 92(11): 5189-5193
- [29] Sritharan M. Iron homeostasis in *Mycobacterium tuberculosis*: mechanistic insights into siderophore-mediated iron uptake[J]. Journal of Bacteriology, 2016, 198(18): 2399-2409
- [30] McMahon MD, Rush JS, Thomas MG. Analyses of MbtB, MbtE, and MbtF suggest revisions to the mycobactin biosynthesis pathway in *Mycobacterium tuberculosis*[J]. Journal of Bacteriology, 2012, 194(11): 2809-2818
- [31] Chao A, Sieminski PJ, Owens CP, Goulding CW. Iron acquisition in *Mycobacterium tuberculosis*[J]. Chemical Reviews, 2019, 119(2): 1193-1220
- [32] Knobloch P, Koliwer-Brandl H, Arnold FM, Hanna N, Gonda I, Adenau S, Personnic N, Barisch C, Seeger MA, Soldati T, et al. *Mycobacterium marinum* produces distinct mycobactin and carboxymycobactin siderophores to promote growth in broth and phagocytes[J]. Cellular Microbiology, 2020, 22(5): e13163
- [33] Krithika R, Marathe U, Saxena P, Ansari MZ, Mohanty D, Gokhale RS. A genetic locus required for iron acquisition in *Mycobacterium tuberculosis*[J]. PNAS, 2006, 103(7): 2069-2074
- [34] Horwitz LD, Horwitz MA. The exochelins of pathogenic mycobacteria: unique, highly potent, lipid- and water-soluble hexadentate iron chelators with multiple potential therapeutic uses[J]. Antioxidants & Redox Signaling, 2014, 21(16): 2246-2261
- [35] Ratledge C, Ewing M. The occurrence of carboxymycobactin, the siderophore of pathogenic mycobacteria, as a second extracellular siderophore in *Mycobacterium smegmatis*[J]. Microbiology: Reading, England, 1996, 142 (Pt 8): 2207-2212
- [36] Jacobs WR Jr, Kalpana GV, Cirillo JD, Pascopella L, Snapper SB, Udani RA, Jones W, Barletta RG, Bloom BR. Genetic Systems for Mycobacteria[M]//Methods in Enzymology. Amsterdam: Elsevier, 1991: 537-555
- [37] Kumar S, Stecher G, Li M, Knyaz C, Tamura K. MEGA X: molecular evolutionary genetics analysis across computing platforms[J]. Molecular Biology and Evolution, 2018, 35(6): 1547-1549
- [38] Johansen MD, Herrmann JL, Kremer L. Non-tuberculous mycobacteria and the rise of *Mycobacterium abscessus*[J]. Nature Reviews Microbiology, 2020, 18(7): 392-407
- [39] Chavadi SS, Stirrett KL, Edupuganti UR, Vergnolle O, Sadhanandan G, Marchiano E, Martin C, Qiu WG, Soll CE, Quadri LEN. Mutational and phylogenetic analyses of the mycobacterial mbt gene cluster[J]. Journal of Bacteriology, 2011, 193(21): 5905-5913
- [40] Shyam M, Shilkar D, Verma H, Dev A, Sinha BN, Brucoli F, Bhakta S, Jayaprakash V. The mycobactin biosynthesis pathway: a prospective therapeutic target in the battle against tuberculosis[J]. Journal of Medicinal Chemistry, 2021, 64(1): 71-100